IOPscience iopscience.iop.org

Home Search Collections Journals About Contact us My IOPscience

Charge dynamics in low-dimensional quantum systems

This article has been downloaded from IOPscience. Please scroll down to see the full text article.

2003 J. Phys.: Condens. Matter 15 S2501

(http://iopscience.iop.org/0953-8984/15/34/303)

View the table of contents for this issue, or go to the journal homepage for more

Download details:
IP Address: 171.66.16.125
The article was downloaded on 19/05/2010 at 15:04

Please note that terms and conditions apply.

INSTITUTE OF PHYSICS PUBLISHING JOURNAL OF PHYSICS: CONDENSED MATTER

J. Phys.: Condens. Matter **15** (2003) S2501–S2511 PII: S0953-8984(03)61773-X

Charge dynamics in low-dimensional quantum systems

B Ruzicka[1], **V Vescoli and L Degiorgi**[2]

Laboratorium für Festkörperphysik ETH-Zürich, CH-8093 Zürich, Switzerland

E-mail: degiorgi@solid.phys.ethz.ch

Received 4 April 2003
Published 15 August 2003
Online at stacks.iop.org/JPhysCM/15/S2501

Abstract

We compare our optical data collected for two families of low-dimensional correlated electron systems: the ladders and the organic Bechgaard salts. Our data display a remarkable optical anisotropy between the spectra along the three crystallographic axes, indicative of the low dimensionality in the electronic band structure. Moreover, we optically identify a dimensionality crossover, induced by Ca doping in the ladders and by chemical pressure in the Bechgaard salts. An outlook on the ongoing research on carbon and MoS_2 nanotubes, as novel one-dimensional quantum wires, is also addressed.

Low-dimensional systems attract a lot of interest, because of the large variety of phenomena they display. While the Fermi liquid (FL) theory has been thoroughly tested on several materials and is usually valid for higher than one dimension, one possible notable exception is the normal state of the two-dimensional (2D) copper oxide-based high-temperature superconductors (HTSC). Recently, a great deal of interest has been devoted to the possible breakdown of the FL framework in quasi-one-dimensional (1D) materials. This is particularly related to the fact that, in a strictly 1D interacting electron system, the FL state is replaced by a state where interactions play a crucial role and which is generally referred to as a Tomonaga–Luttinger liquid (TLL) [1]. This novel quantum state in condensed matter recently led to a wealth of both experimental and theoretical studies in materials, which can be characterized as prototype low-dimensional quantum systems (like the organic 1D chain Bechgaard salts or the ladders), as well as in nanostructured specimens (like the 1D quantum wire based on carbon and molybdenum disulfide nanotubes).

Even-leg spin-ladder systems, like the $Sr_{14-x}Ca_xCu_{24}O_{41}$ series, have attracted much interest since Dagotto *et al* [2] first suggested that they should have a spin liquid ground state with a spin gap and that doping (e.g. by Ca substitution) would result in pairing of

[1] Present address: Dipartimento di Fisica, Università La Sapienza Roma, Piazza Aldo Moro 2, I-00185 Rome, Italy.
[2] Author to whom any correspondence should be addressed.

 © 2003 IOP Publishing Ltd Printed in the UK

the doped holes with a charge density wave (CDW) or superconducting ground state [2, 3]. The existence of a spin gap in this new class of compounds has been clearly shown by NMR [4, 5] and inelastic neutron scattering [6], while superconductivity has been found in $Sr_{0.4}Ca_{13.6}Cu_{24}O_{41.84}$ [7] and $Sr_{2.5}Ca_{11.5}Cu_{24}O_{41}$ [8] when a pressure greater than 3 GPa is applied. In a much broader perspective, the discovery of superconductivity in the ladders revived interest in the superconductivity in two families of materials where this property was not expected at first sight: low-dimensional organic conductors, like the Bechgaard salts (i.e. $(TMTTF)_2X$ or $(TMTSF)_2X$ with $X = PF_6$, Br and ClO_4), and the high-temperature cuprates. The mechanism of superconductivity in the ladders is still under intense debate, but it seems to be correlated to the low-dimensional electronic structure as well. Transport and optical measurements have, in fact, shown that these systems are highly anisotropic along the three crystallographic axes [9–16].

In this brief report, we review the light polarization dependence of the electrodynamic response of single crystalline $Sr_{14-x}Ca_xCu_{24}O_{41}$ (with $x = 0$, 5 and 12). Our motivation is to monitor the effects of the reduced dimensionality (i.e. the crystallographic anisotropy) on the excitation spectrum of the ladder systems [10] and to compare the ladder's optical properties with those of the organic Bechgaard salts, investigated over the past few years [11, 12]. We shall also briefly address some recent optical data on carbon as well as on MoS_2 nanotubes.

For the organic and ladder compounds we used single crystals, grown following the procedures described in the literature [10–13]. The optical reflectivity $R(\omega)$ was measured as a function of temperature over a broad spectral range from 4 meV up to 12 eV, using four different spectrometers, and for light polarization parallel and perpendicular to the ladder direction in the ladder planes, and orthogonal to the ladder planes [10]. For the Bechgaard salts, the light was polarized parallel and perpendicular to the chain axis [11, 12]. The optical conductivity was obtained from Kramers–Kronig transformations of the measured reflectivity [10–12].

Figure 1 shows the $R(\omega)$ spectra along ($E \parallel c$) and perpendicular ($E \parallel a$) to the ladder direction in the ladder planes for the undoped sample ($x = 0$) and for the doped sample ($x = 5$ and 12) at $T = 300$ K [10]. Our spectra along the ladder direction are in good agreement with the data collected by Osafune *et al* [14]. $R(\omega)$ increases with decreasing photon energy for both compounds and directions, and approaches total reflection as ω tends to zero, as expected for metallic behaviour. In passing, we shall mention that an insulating behaviour (i.e. $R(\omega)$ saturating to a constant value) is instead observed at $T = 10$ K for $x = 0$, while $R(\omega)$ for $x = 12$ decreases in the far-infrared with decreasing temperature but still displays a metallic-like behaviour [10]. We can also identify a plasma edge feature in the reflectivity, defined by the minimum in $R(\omega)$ where the onset for the increase towards total reflection takes place. Such an onset of the metallic contribution in $R(\omega)$ for $E \parallel c$ is centred at about 0.5 eV for the less conducting composition ($x = 0$) and shifts towards higher energies with high Ca substitution ($x = 5$ and 12). For $E \parallel a$, a plasma edge-like behaviour is clearly seen only for $x = 12$ (see below). At higher frequencies there are several broad absorptions, ascribed to electronic interband transitions, like the one, peaked at about 2 eV, due to a charge transfer excitation between Cu 3d and O 2p states [14]. In order to highlight the optical anisotropy, we also show in figure 1(c) $R(\omega)$ for $x = 12$ along the three crystallographic axes at $T = 300$ K. Along the direction orthogonal to the ac plane (i.e. b axis), $R(\omega)$ is always insulating-like and temperature-independent for all Ca substitution values (also for $x = 0$ and 5, not shown here). Moreover, all spectra are dominated by rather sharp absorptions in the far- to mid-infrared range, which are ascribed to phonon modes.

The optical properties are very anisotropic, with distinct temperature and polarization dependences along the three crystallographic axes [10]. More recent data by Osafune *et al* [15] confirm the optical anisotropy previously found in our spectra, even though along the c axis the

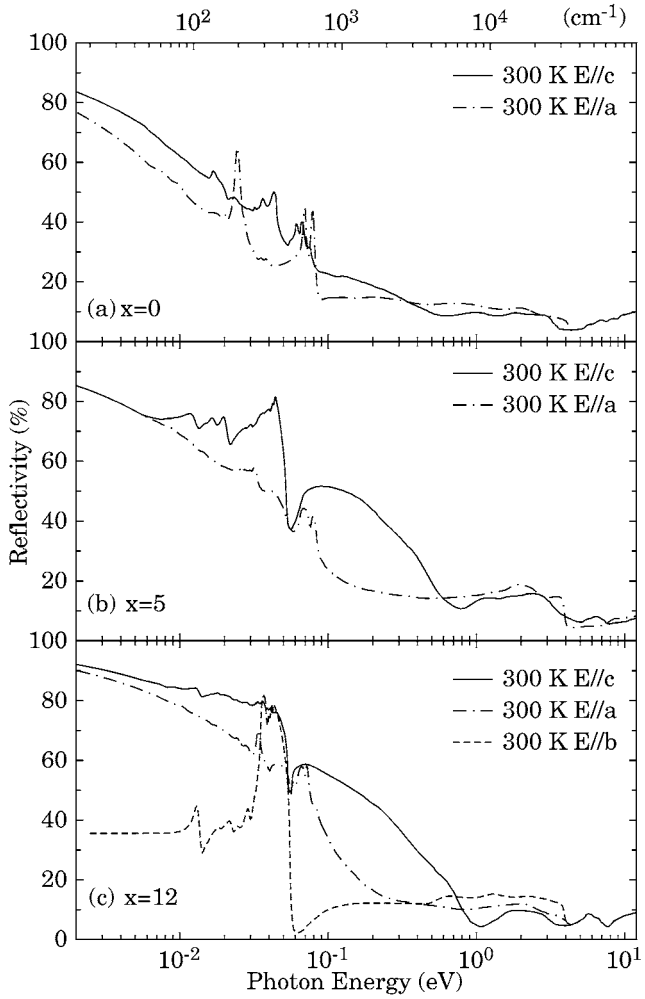

Figure 1. Optical reflectivity of $Sr_{14-x}Ca_xCu_{24}O_{41}$ at $T = 300$ K along the c and a axes for $x = 0$ (a), $x = 5$ (b) and $x = 12$ (c). Panel (c) also displays $R(\omega)$ at 300 K along the b axis for $x = 12$. Note the logarithmic energy scale [10].

same group suggests the presence of a collective mode at low frequencies and temperatures, for which we do not have clear cut evidence. The reason for this disagreement is at present unknown but it is not relevant for this discussion.

The strong optical anisotropy in the ladders implies a low-dimensional electronic structure. At this point, it is interesting to make a comparison with the quasi-1D Bechgaard salts [11, 12]. The Bechgaard salts are highly anisotropic systems, with transfer integrals along the three crystallographic axes approximately given by t_a:t_b:t_c = 250:10:1 meV for the (TMTTF) family and by t_a:t_b:t_c = 250:25:1 meV for the TMTSF one (where here the convention for the axes assignment is: a for the chain axis, b and c for the intermediate and least conducting axis, respectively). The optical anisotropy is evident in figure 2 where reflectivity measurements for two representative members of the two classes of salts (i.e. $(TMTTF)_2Br$ and $(TMTSF)_2PF_6$, respectively) along the three crystallographic axes (i.e. $E \parallel a$ and $E \parallel c$ (a) and $E \parallel b$ (b)) at different temperatures are shown. Going from the (TMTTF) to the (TMTSF) salts one can

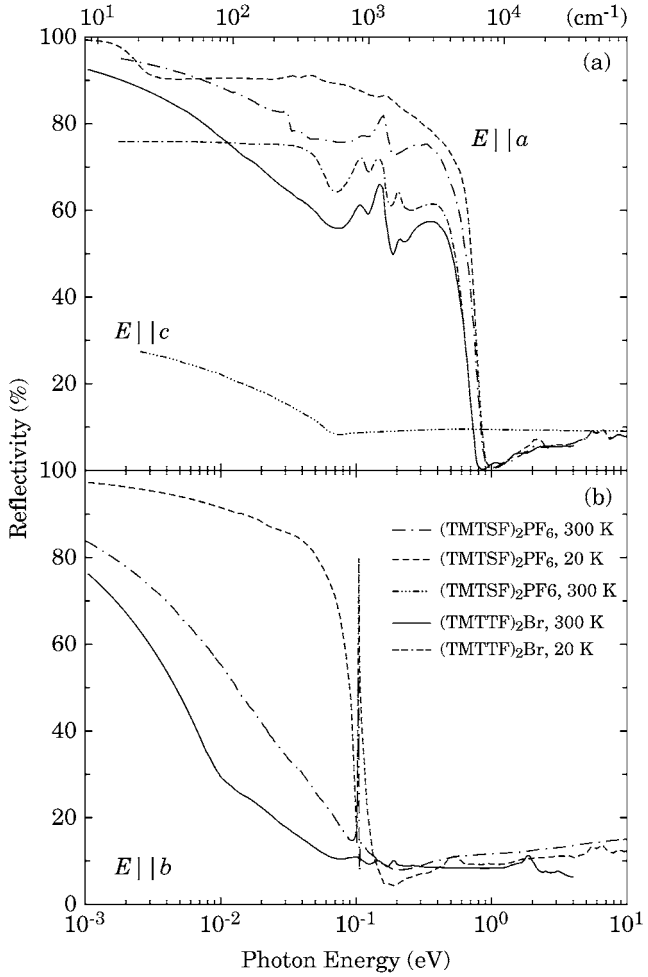

Figure 2. Optical reflectivity (a) along the a and c directions and (b) along the b direction for $(TMTTF)_2Br$ and $(TMTSF)_2PF_6$ at $T = 300$ and 20 K. Note the logarithmic energy scale [11, 12].

observe an insulator to metal transition at 20 K. For the TMTTF Bechgaard salts electron–electron interactions and Umklapp scattering lead to an insulating state, characterized by a correlation gap in the charge excitation spectrum (see below) [11, 12]. In fact, the reflectivity of the TMTTF salt is insulating-like (i.e. $R(\omega)$ saturates to a constant value for $\omega \to 0$) along the chain axis (figure 2(a)) and displays an overdamped-like (i.e. the Drude scattering rate is much larger than the plasma frequency) and temperature-independent behaviour along the b axis (figure 2(b)). On the other hand, for the (TMTSF) family the chain axis reflectivity is metallic-like at any temperatures (figure 2(a)), while along the b axis there is a clear evolution from the overdamped-like behaviour of the plasma edge to a sharp plasma edge feature with decreasing temperature (figure 2(b)). Along the c axis $R(\omega)$ remains insulating-like at any temperatures (figure 2(a)).

Figure 3 summarizes the temperature dependence of the real part $\sigma_1(\omega)$ of the optical conductivity in different Bechgaard salts for $E \parallel a$, the chain's direction. Parts (a) and (b) show $\sigma_1(\omega)$ for the PF_6 and Br compounds of the TMTTF family, while part (c) displays

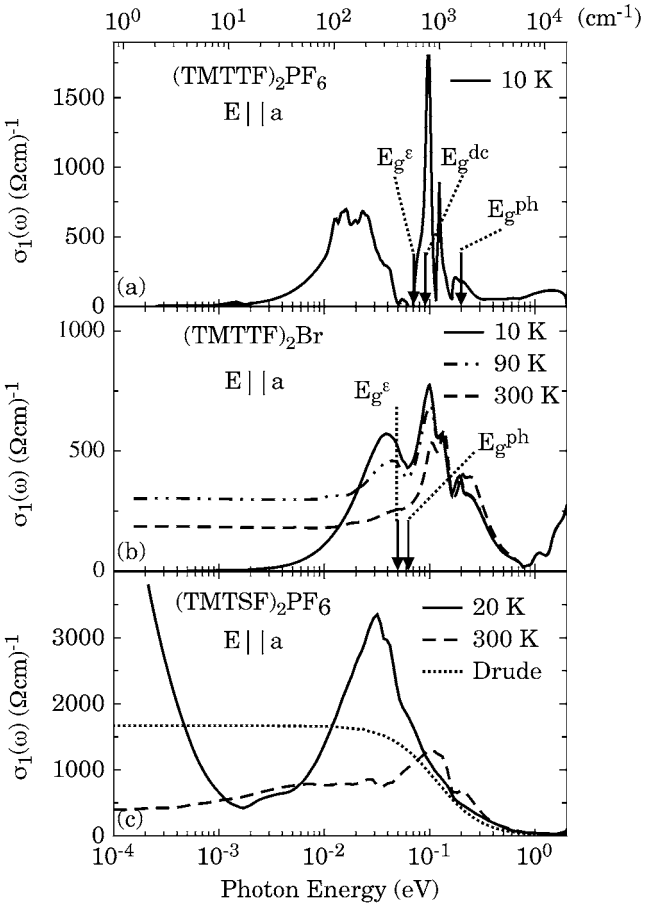

Figure 3. On-chain optical conductivity of (a) $(TMTTF)_2PF_6$, (b) $(TMTTF)_2Br$ and (c) $(TMTSF)_2PF_6$ at temperatures above the transitions to the broken symmetry states. The arrows indicate the gaps observed by dielectric (ε) response, dc resistivity and photoemission (ph). A simple Drude component is also shown in part (c). Note that photoemission measures the quantity $E_g/2$, assuming that the Fermi level is in the middle of the gap [12].

$\sigma_1(\omega)$ for $(TMTSF)_2PF_6$. We can immediately remark that the temperature dependence of $\sigma_1(\omega)$ is quite important in all compounds, except in $(TMTTF)_2PF_6$, which is basically in an insulating state at all temperatures. The optical conductivity of the TMTTF salts displays several transitions with large absorption features due to lattice vibrations (phonon modes), mainly due to the inter- and intramolecular vibrations of the TMTTF (and TMTSF) unit. The phonon modes are particularly observed in the TMTTF salts, because the screening by free electrons is less effective. Although it is clear that the optical properties of the TMTTF salts are those of a semiconductor, with a gap for the charge excitations, the identification of the gap, based on the optical spectra, is not straightforward, because of the large phonon activity. Thus, the results of other measurements were used to evaluate the gap (see the arrows in figure 3 and [11] and [12] for details). Because the band is partially filled, the charge gap in both of the $(TMTTF)_2X$ salts is a correlation rather than a single-particle gap. Such a correlation gap can be shown within a Mott–Hubbard scenario of quasi-1D (Luttinger liquid) systems, taking also into account the Umklapp scattering mechanism [12].

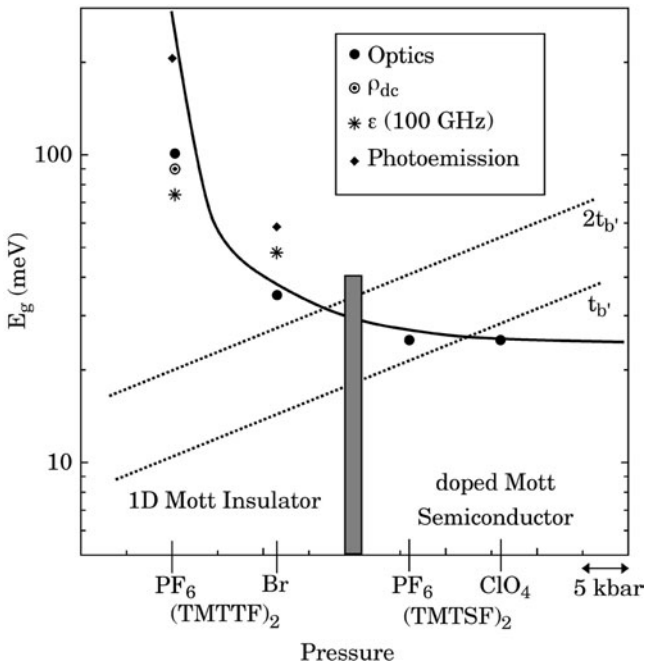

Figure 4. The pressure dependence of the (Mott) correlation gap (E_g), as established by different experimental methods, and of the transfer integral, perpendicular to the chains, t_b, for the Bechgaard salts. The horizontal scale was derived with the results of pressure studies [11, 12, 17].

The optical properties of the $(TMTSF)_2X$ analogues, for which the dc conductivity gives evidence for metallic behaviour down to low temperatures (to the transition to the spin density wave state at T_{SDW}), are markedly different from those of a simple metal. A well-defined gap feature around 25 meV and a zero-frequency mode are observed at low temperatures. The combined spectral weight of the two modes is in full agreement with the known carrier concentration of 1.4×10^{21} cm^{-3} and a band mass that is very close to the electron mass [11]. For both $(TMTSF)_2X$ salts, the zero-frequency mode has small spectral weight of the order of 1% of the total. Nevertheless, this mode is responsible for the large metallic conductivity. The feature at 25 meV is ascribed to the so-called charge correlation pseudogap [11, 12].

It has been suggested that the insulator–metal phase transition, taking place between the TMTTF and TMTSF families of Bechgaard salts, is driven by a dimensionality crossover [11, 12]. Such a transition occurs when the transverse charge transfer integral t_b is comparable or exceeds the Mott–Hubbard charge correlation gap (E_g) [11, 12]. The dimensionality crossover, induced by the increasing t_b upon pressure or by changing the chemistry from the TMTTF to the TMTSF family, is one of the central issues. There is a well-established order for t_b among the four salts investigated, as mentioned above. To arrive at a scale for t_b, we took the calculated values within the tight-binding model as averages for the $(TMTSF)_2X$ and $(TMTTF)_2X$ salts, respectively, and assumed that pressure changes t_b in a linear fashion. The positions of the various salts along the horizontal axis of figure 4 reflect this choice [11, 12], with pressure values taken from the literature; such a scale has been widely used when discussing the broken symmetry ground states of these materials [17].

The full curve in figure 4 represents the overall behaviour of the correlation gap. Various experiments give slightly different values of the gap (see also figure 3). This is probably

due to the differences in the curvature of the band, which is scanned differently by different experiments, or due to the different spectral response functions involved. The dotted curve representing $2t_b$ (this is half the bandwidth perpendicular to the chains in the tight-binding approximation) crosses the full curve displaying the behaviour of E_g between the salts exhibiting insulating and metallic behaviour, whereas the dotted line representing t_b crosses the full curve between the two metallic salts. Therefore, our experiments strongly suggest that a crossover from a non-conducting (Mott insulator) to a conducting state (doped Mott semiconductor) occurs when the unrenormalized single-particle transfer integral between the chains exceeds the correlation gap by a factor, which is of the order of but somewhat greater than 1 (figure 4). For TMTTF salts the electrons are confined on the chain ($t_b < E_g$), while for TMTSF salts deconfinement is possible ($t_b > E_g$). The evolution from the confinement to the deconfinement regime is a clear indication of the dimensionality crossover from a 1D Mott insulator to a quasi-2D FL metal, under the effect of increasing transverse (i.e. perpendicular to the 1D chains) interactions [11]. Such a crossover can also be obtained in the (TMTTF)-salts upon application of pressure [16].

Additional evidence for a pronounced qualitative difference between states with $t_b < E_g$ and $t_b > E_g$ is given by plasma frequency studies along the b direction (i.e. perpendicular to the chain). As shown in figure 2(b), there is no well-defined plasma frequency for the insulating state of the TMTTF salts, and we regard this as evidence for the confinement of electrons on individual chains. In fact, the reflectivity has a temperature-independent overdamped-like behaviour. Conversely, the electrons become deconfined as soon as $t_b \sim E_g$ (figure 4). Such a deconfinement is manifested by the onset of a sharp plasma edge in the low-temperature reflectivity spectra of the (TMTSF) salts along the b axis (figure 2(b)). This conclusion is not entirely unexpected: a simple argument (the same as one would advance for a band-crossing transition for an uncorrelated band semiconductor) would suggest that, to create an electron–hole pair with the electron and hole residing on neighbouring chains, an energy comparable to the (charge correlation) gap would be required. This is equivalent to a scenario where the deconfinement caused by the interchain coupling (t_b) effectively induces a so-called self-doping of the system (i.e. the doped Mott semiconductor, mentioned above) [11, 12].

Based on these arguments developed for the organic linear chain systems, we can now argue that in ladder systems as well a similar dimensionality crossover can be recognized. In fact, from our data in figure 1 we observe that the increasing Ca substitution induces the formation of a well developed plasma edge feature in $R(\omega)$ along both the a and c axes. This is actually to be expected along the c axis, because holes of the CuO_2 chains reservoir are transferred to the ladder conduction paths upon Ca substitution [14]. Moreover, one can observe an increased metallicity upon doping also along the transverse direction (a axis in figure 1, which is equivalent to the b direction in the Bechgaard salts), manifested by an incipient plasma edge feature. This bears a remarkable analogy with the behaviour in Bechgaard salts (figure 2(b)) and indicates a similar confinement–deconfinement crossover upon Ca substitution.

The analogy between ladder systems and Bechgaard salts has already been pointed out by Mayaffre *et al* [18]. The degree of confinement of the carriers along the ladders could correlate with the size of the spin gap: hole pairs are responsible for the conduction within the ladders as long as the magnetic forces can provide the binding of two holes on the same rung [2]. The vanishing of the spin gap upon application of pressure [18] or its reduction upon Ca substitution could be responsible for the dissociation of the pairs, making the hopping (deconfinement) of the transverse single particle easier. Therefore, pressure is believed to have an effect similar to that of Ca substitution and, similarly to the Bechgaard salts, might induce a change in the intrinsic dimensionality of the system. It turns out that Ca substitution can be regarded as a chemical pressure because of its smaller ionic radius, leading to lattice

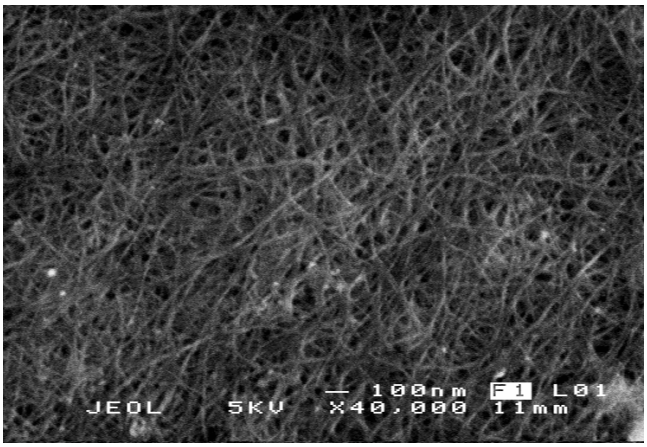

Figure 5. SEM image of the pristine SWNT thick film used in dc transport and optical conductivity measurements [23].

contraction, and its major effect on the ladders is to increase the hole density [8]. Nagata *et al* [8] also suggest that the application of pressure on ladder systems triggers a dimensional crossover from one to two due to the enhancement of interladder interactions. Therefore, pressure is even more important than doping since the increased pressure induces not only superconductivity but also coherent charge dynamics perpendicular to the ladders.

In order to broaden the perspectives and as an outlook on future developments, we shall briefly mention here the ongoing activity on carbon nanotubes, which have been discovered in carbon rods after an arc discharge by high-resolution transmission electron microscopy [19]. A needle typically consists of a few microtubules centred coaxially about the needle axis, and is hollow. A microtubule has the form of a rolled graphitic sheet with a diameter of a few nanometres. A lot of interest in such a new form of carbon is also associated with the possible and potentially interesting technical applications and uses. A partial list includes: superstrong cables, wires for nanosized electronic devices, charge-storage devices in batteries, and tiny electron guns for flat-screen televisions [20].

It is expected that the graphitic microtubules exhibit a variety of properties in electronic conduction, from a typical semiconductor to a good metal, depending on the tubule structure, i.e. chirality [21]. The tubule morphology suggests that these systems should represent a fascinating class of novel quasi-1D structures and can be considered as the ultimate realization of a 1D quantum wire. The typical signatures of the quasi-1D nature of the electronic properties were also identified in metallic single-walled nanotubes (SWNT) [22].

Figure 5 shows the scanning electron microscopy (SEM) image of the pristine sample [23]. The sample consists of a high density of SWNT ropes of different diameters with a very low density of impurities. Due to the preparation method of the bucky paper by depositing it on a filtration membrane, the bucky paper quality is quite reproducible. The density is in the 40 mg cm^{-3} range (the theoretical density of the rope is 1.3 g cm^{-3}). This can vary slightly from batch to batch, and consequently the bucky paper resistivity too. However, the dc and optical conductivity were measured on the same bucky paper. The dc properties, shown in the inset of figure 6, were obtained with the conventional four-points contact method. The optical conductivity was measured in a broad spectral range, similar to our previous experiments on organic chain salts and ladders, through Kramers–Kronig transformation of the reflectivity spectra of the specimen shown in figure 5 [23].

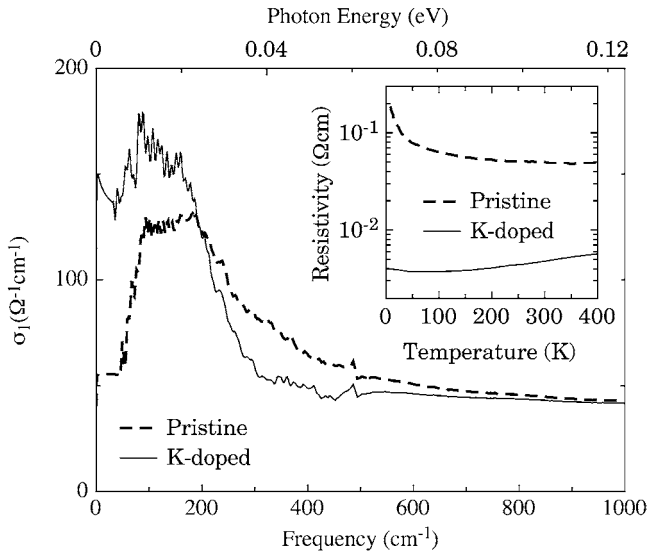

Figure 6. Optical conductivity as a function of wavenumber (photon energy) for pristine and K-doped SWNT sample. The inset displays the dc resistivity for both the pristine and K-doped SWNT [23].

Figure 6 displays the real part $\sigma_1(\omega)$ of the optical conductivity for the pristine and K-doped SWNT samples at $T = 300$ K. In all measured samples we did not find any temperature dependence in the optical spectra, in agreement with the weak temperature dependence of the resistivity (inset of figure 6). We also note that the bucky paper thickness of about 20 μm was large enough so that our samples were not transparent in the investigated frequency range. In fact, the samples were mounted either on a Cu or on a glass plate and no contribution from or interference effects due to the bucky paper substrate were found. For both samples the reflectivity increases for decreasing frequency from the visible down to the FIR range, showing the typical optical fingerprint for metallic behaviour, with a plasma edge at about 2000 cm^{-1} [23]. However, for the doped sample a further increase of reflectivity in the mid- and far-infrared region (at frequencies lower than 400 cm^{-1}) is evident, signalling the appearance of a stronger free charge carrier contribution (Drude component in the optical conductivity) at very low frequencies (figure 6). This is pretty much in agreement with the dc properties (inset of figure 6), showing a reduced resistivity upon K doping. While our previous optical investigations on multi-walled carbon nanotube films (where the tubes were mechanically aligned) revealed the anisotropy of the charge dynamics [24], the present data on SWNT display characteristic optical fingerprints of a quasi-1D system. Indeed, a broad bump at about 200 cm^{-1} is also evident for both samples [23]. This is ascribed to a (Mott–Hubbard) charge correlation gap [23]. The similarity with the organic linear chain Bechgaard salts is striking and these data on novel 1D quantum wires reinforce a scenario, where 1D materials are on the verge of a Mott insulating state and might be appropriately driven into a (anomalous) conducting phase by doping and/or upon increasing the intrinsic dimensionality of the electronic structure (by chemical or applied pressure).

Finally, we also would like to mention another class of tubular structures consisting of the tungsten and molybdenum disulfide (WS_2 and MoS_2) materials [25, 26]. Synthesis of such nanotubes made of atoms other than carbon may be possible and tubes as small as 15 nm have

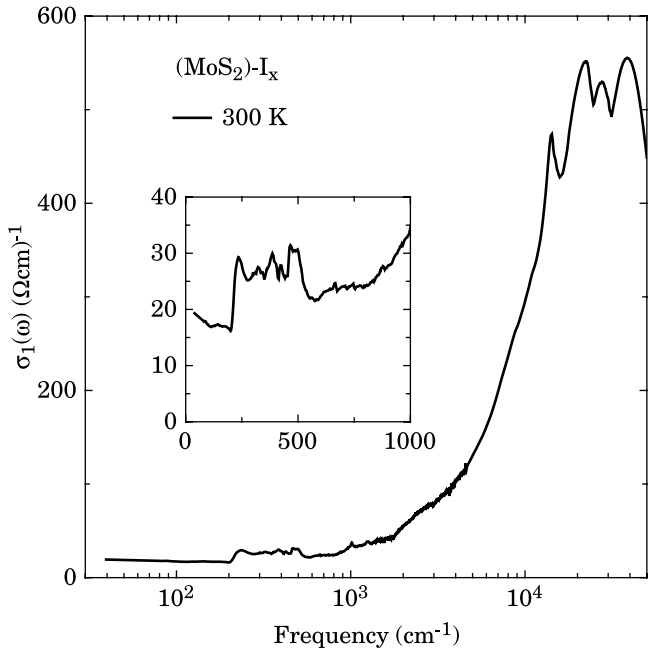

Figure 7. Real part $\sigma_1(\omega)$ of the optical conductivity of (MoS_2)–I_x. The inset highlights the infrared spectral range. One can observe the finite dc limit of $\sigma_1(\omega)$ which indicates the presence of Drude weight.

been found. The efficient synthesis of identical single wall MoS_2 nanotubes is expected to lead the way to the synthesis of other related dichalgogenide systems, even in the sub-nanometre range. This will open new perspectives and will facilitate the investigation of truly single-tube properties and related quantum effects.

Our first optical investigations were performed on (MoS_2)–I_x specimens [26]. The single-wall MoS_2 nanotubes were grown by a catalyzed transport method using C_{60} as a growth promoter and iodine as the transport agent. Energy-dispersive x-ray spectroscopy and x-ray fluorescence spectrometry have shown the chemical composition of the bundles to be (MoS_2)–I_x with $x \sim 1/3$. A structure consisting of sulfur–molybdenum–sulfur cylinders with the so-called (3, 3) armchair nanotube configuration was proposed [26]. Figure 7 displays the optical conductivity $\sigma_1(\omega)$ from the far-infrared up to the ultraviolet, while the inset enhances the absorption features in the infrared spectral range. Recently, large-diameter armchair MoS_2 nanotubes were predicted on the basis of density-functional tight binding calculations [27] to be semiconducting with either a direct or an indirect bandgap, depending on their diameter and structure. For the tubes discussed here one can expect the indirect gap to close, giving rise to a metal with a small, but finite, density of states at the Fermi level [26]. This seems to be indeed confirmed by our data (figure 7) which clearly indicate the presence of a small amount of Drude weight and a finite dc limit of $\sigma_1(\omega)$ (inset of figure 7). The reflectivity (not shown here and to be reported elsewhere) is characterized by a rather overdamped-like behaviour of its plasma edge and can be extrapolated at low frequencies towards zero with the usual Hagen–Rubens extrapolation. Nevertheless, the effect of the confinement of electrons in the very narrow tubes might be expected to give rise to energy level quantization. In order to shed more light on this issue, optical investigations along different polarization directions are

desired. These investigations are in progress and will allow us to understand the still puzzling, and in many respects controversial, results on 1D quantum wires in general.

In summary, the electrodynamics of $Sr_{14-x}Ca_xCu_{24}O_{41}$ provides strong evidence for the low dimensionality of the ladder systems, manifested by the anisotropic optical response. Upon Ca substitution, there is a progressive deconfinement of the pre-formed hole pairs and a crossover from a 1D to a 2D electronic structure. We have stressed the similarities with another class of correlated low-dimensional systems, namely the organic Bechgaard salts. Novel 1D systems, like the carbon and WS_2 and MoS_2 nanotubes, are nowadays under investigation and are opening up new perspectives for our understanding of highly correlated systems in low dimensions.

Acknowledgments

We wish to thank U Ammerahl, A Revcolevschi, L Forro, D Mihailovic and L K Montgomery for supplying well-characterized samples, and T Giamarchi, E Dagotto, D Jerome and G Gruner for fruitful discussions. This work has been financially supported by the Swiss National Foundation for the Scientific Research.

References

[1] For a review, see
Schulz H J 1991 *Int. J. Mod. Phys.* B **5** 57
[2] Dagotto E *et al* 1992 *Phys. Rev.* B **45** 5744
[3] Dagotto E and Rice T M 1996 *Science* **271** 618
[4] Magishi K *et al* 1998 *Phys. Rev.* B **57** 11533
[5] Tsuji S *et al* 1996 *J. Phys. Soc. Japan* **65** 3474
[6] Eccleston R S *et al* 1998 *Phys. Rev. Lett.* **81** 1702
[7] Uehara M *et al* 1996 *J. Phys. Soc. Japan* **65** 2764
[8] Nagata T *et al* 1998 *Phys. Rev. Lett.* **81** 1090
[9] Motoyama N *et al* 1997 *Phys. Rev.* B **55** R3386
[10] Ruzicka B *et al* 1998 *Eur. Phys. J.* B **6** 301
[11] Vescoli V *et al* 1998 *Science* **281** 1181
[12] Vescoli V *et al* 2000 *Eur. Phys. J.* B **13** 503
[13] Revcolevschi A and Jegoudez J 1996 *Coherence in High Temperature Superconductors* ed G Deutscher and A Revcolevschi (Singapore: World Scientific) p 19
[14] Osafune T *et al* 1997 *Phys. Rev. Lett.* **78** 1980
[15] Osafune T *et al* 1999 *Phys. Rev. Lett.* **82** 1313
[16] Moser J *et al* 1998 *Eur. Phys. J.* B **1** 39
[17] Jerome D and Schulz H J 1982 *Adv. Phys.* **31** 299
[18] Mayaffre H *et al* 1998 *Science* **279** 345
[19] Iijima S 1991 *Nature* **354** 56
[20] Service R F 1998 *Science* **281** 940
[21] Blase X *et al* 1994 *Phys. Rev. Lett.* **72** 1878
[22] Bockrath M *et al* 1999 *Nature* **397** 598
[23] Ruzicka B *et al* 2000 *Phys. Rev.* B **61** R2468
[24] Bommeli F *et al* 1996 *Solid State Commun.* **99** 513
[25] Tenne R *et al* 1992 *Nature* **360** 444
[26] Remskar M *et al* 2001 *Science* **292** 479
[27] Siefert G *et al* 2000 *Phys. Rev. Lett.* **85** 146